

1. Proposal Overview and Objectives

The distribution of deformation within the lithospheric mantle beneath the San Andreas fault system is not presently well constrained. Determining the geometry of deformation of the ductile portion of the fault system has important implications for our understanding of lithospheric mantle rheology and can provide constraints on whether block models can be considered as a reasonable approximation throughout the width of the entire lithosphere. The purpose of our study was to provide preliminary observational constraints on the geometry of the ductile portion of the San Andreas fault system in southern California, and to compare these results to those calculated for central California. Ps receiver function analysis was used in order to image lateral variations in anisotropy within the lithosphere, both crust and mantle, in southern California at 6-8 permanent station locations, in order to identify where plate boundary deformation related to the SAF system is located. Specific objectives that we intended to address in our study included 1) characterizing changes in the orientation of seismic anisotropy change from the lithosphere to the asthenosphere in southern California, 2) determining whether lateral variations in seismic anisotropy exist within the lithosphere across the plate boundary and 3) comparing our results to those in central California.

2. Background

Today ~75% of the relative motion between the North American and Pacific plates is accommodated by the San Andreas fault (SAF) system (Molnar and Dayem, 2010; Rolandone et al., 2008) with the residual accommodated by deformation in the Walker Lane region, east of the Sierra Nevada (e.g., Wesnousky et al., 2012). While the expression of the SAF system at the surface and shallow crustal depths is relatively well constrained the geometry of the plate boundary and associated deformation at lithospheric mantle depths remains unclear. CCP stacked Sp receiver functions imaged systematic, lateral variations in the strength of the shear wave velocity gradient from lithosphere to asthenosphere that are coincident with the surface expression of the SAF (Ford et al., 2014). In some regions, such as central California, the changes in lithosphere-asthenosphere boundary (LAB) strength occur over a horizontal length scale of less than 50 km. The correlation between the surface expression of the central SAF and the laterally abrupt change in velocity structure of the basal mantle lithosphere points to the accommodation of relative plate motion on a narrow shear zone (< 50 km in width) that extends throughout the entire thickness of the lithosphere. In contrast, lateral variations in the strength of the LAB in southern California appear to be more gradual, suggesting that the zone of deformation may be distributed.

The presence of seismic anisotropy in the mantle is typically the result of the lattice-preferred orientation of olivine via dislocation creep. In the western U.S., dense regional networks, in addition to temporary deployments such as Earthscope, have provided us with voluminous data sets useful for conducting analysis of seismic anisotropy. Results from this region have shown evidence for complex patterns of seismic anisotropy, evidenced by rapid changes in fast-axis direction over short lateral distances (e.g., Eakin et al., 2010; Lin et al., 2010; Barak and Klemperer, 2016). However, a significant limitation of such methods is that seismic anisotropy is integrated along the ray path from the core-mantle boundary to the surface, making it difficult to resolve layered structure. An alternative analysis tool that can provide firm constraints on the presence of anisotropic boundaries is Ps receiver function analysis (e.g., Bostock, 1998; Levin and Park, 1997; Savage, 1998). Provided an accurate velocity model, uncertainties in depth are on the order of a couple kilometers (Abt et al., 2010) for the technique, and thin layers of less than 8-10 km can be resolved (Leahy and Park, 2005).

Shear wave splitting has been used to invoke two different models of deformation along the SAF plate boundary. In central California, Bonnin et al. (2010) argued for a relatively narrow shear zone at the base of the mantle lithosphere. Bonnin et al. (2012) also concluded that the anisotropic boundary between lithosphere and asthenosphere was abrupt, something that can be tested with Ps receiver function analysis. Monteiller and Chevrot (2011) came to a very different conclusion in southern California. There they

found that there is no well-defined shear zone and concluded that deformation is diffuse and centered beneath the Eastern California Shear Zone.

3. Methods and Data

Ps receiver function analysis is a seismic imaging technique that is used to identify discontinuity structure in the crust, upper mantle and mantle transition zones. The technique uses the partial scattering of a primary P-phase at a boundary in seismic properties, into an S-wave, respectively, to infer information (i.e., depth, impedance contrast, seismic anisotropy) about the scatterer. The behavior of Ps receiver functions in the presence of anisotropy has been well documented (e.g., Fredericksen and Bostock, 2000; Levin and Park, 1997; Savage, 1998) and used to confirm the existence of anisotropic structure in a number of tectonic settings (e.g., Bostock, 1998; Schulte-Pelkum et al., 2005; Porter et al., 2011; Yuan and Levin, 2014; Ford et al., 2016). In an isotropic Earth (with no dipping structure), coupling occurs between P and SV wave motion, with the P-SV system remaining decoupled from SH wave propagation. When anisotropy and/or dipping structure is present, coupling occurs among P, SV, and SH waves. In such cases, calculating the transverse component receiver function can alert us to the presence of anisotropy and/or dipping structure. A key aspect of anisotropic receiver function analysis is the nature of the variation in back azimuth produced by anisotropic structure (e.g., Levin and Park, 1998). In the presence of horizontally oriented anisotropy, the amplitude variations with back azimuth follow a four-lobed pattern in the radial and transverse receiver functions. Anisotropy with a tilted axis, or an isotropic dipping interface, produces a two-lobed pattern.

Anisotropic Ps receiver function analysis has been successfully used in the past to constrain the presence of anisotropy in the crust in both central and southern California. Porter et al. (2011) modeled receiver functions and compared results to data from southern California and determined that the patterns of anisotropy observed in the results could be best explained by the regional underplating of schists; a similar conclusion was reached by Schulte-Pelkum and Mahan (2014). Further to the north at station PKD in central California, a similar trend was seen by Ozacar and Zandt (2009), who also used the underplating of schists to explain their results within the crust.

Initial results prior to the start of the study were compiled for central California, from the stations shown in **Figure 1**. These stations were selected in order to look for systematic changes in seismic anisotropy across the Pacific-North American plate boundary. While our study was originally intended to focus on the anisotropy of the lithosphere-asthenosphere boundary in southern California, *our report focuses on our results of the Walker Lane area*, and more specifically on changes in anisotropy at the Moho and in the uppermost mantle, which prove most compelling and are currently the subject of follow-up work and manuscript preparation. Initial processing of the downloaded data included waveform windowing, rotation (into the R, T, Z reference frame) and filtering (0.2 to 2 Hz). Waveforms were visually inspected for an unambiguous P wave arrival on the vertical and clear radial and transverse components using PQL and the direct P arrival for each event was manually picked using the SAC (top right). Receiver functions were calculated using a frequency domain multitaper correlation technique, referred to here as the multitaper method (MTM) (Park and Levin, 2000). The MTM is achieved using a least squares correlation between the eigenspectral of the R, T, and Z. Before RF computation, waveforms were band-pass filtered with a high-pass cutoff of 0.02 Hz and a low-pass cutoff of 0.5, 0.75, 1.0, 1.5 and 2 Hz (in separate sets of calculations). After the individual RFs were calculated, they were corrected for variations in slowness (i.e., epicentral distance) and stacked. Radial and transverse component RFs were binned as a function of epicentral distance and back azimuth (bottom right), using a bin spacing of 5° and 10°, respectively. Within each bin the individual RFs were weighted according to their uncertainties, which were estimated by the coherence. Figure 2 provides examples of three receiver functions

4. Results

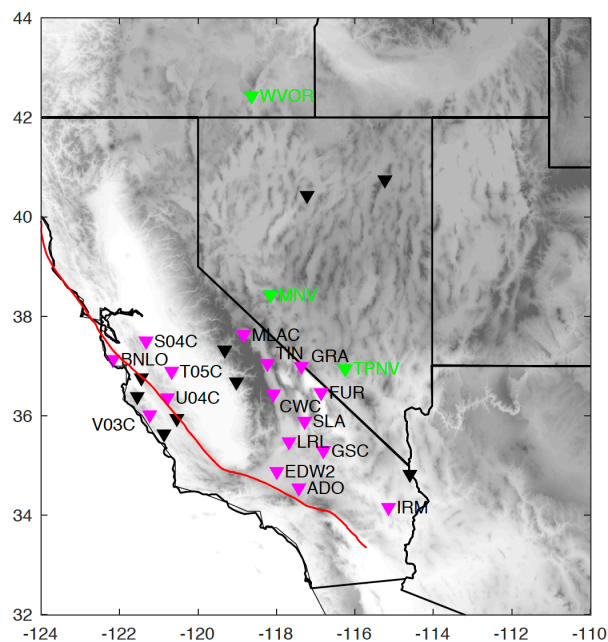


Figure 1. Map of station locations where P_s receiver functions (RFs) were calculated either in this study or previously. Black inverted triangles correspond to stations where P_s RFs were previously calculated and are not discussed in this report. Inverted green triangles are stations where P_s RFs were previously calculated and are shown in **Figure 2**. P_s RFs for stations calculated in this study are shown in magenta. P_s RFs for stations GRA, FUR and SLA are shown in **Figure 2**.

The initial analysis, which included data processing and computation of receiver functions was carried out by three undergraduate students at the University of California, Riverside as part of the course GEO 190 (Special Studies). Each student was given a geographic region to focus on were closely supervised by the PI and graduate students within the PIs lab. The geographic regions were: central California near the San Andreas fault, Mojave Desert, and Walker Lane (**Figure A**). Generally speaking, results from coastal central California and results from Walker Lane, appeared reasonable, if in some places complex. This is primarily based on the observation that large, robust positive phases are seen at ~ 4 -6 seconds on the radial component, which agrees well with estimates of Moho arrival times for the region (**Figure 2**). A large amplitude negative phase thought to be associated with scattering from the lithosphere-asthenosphere boundary is also observed on the radial component at ~ 8 -12 seconds (**Figure 2**) at most stations. Results from stations in the Mojave (ADO, EDW2, LRL, GSC and IRM) did not exhibit clear Moho and LAB signals, indicating a potential issue with the computation of the receiver functions (initial processing and phase picking appears to be correct). The PI and graduate student are currently working to recalculate receiver functions for the Mojave region.

Figure 2 presents the highlight of our research results for the Walker Lane region. While the study was initially conceived to characterize changes in anisotropy across the Pacific-North America plate boundary, the defining feature of our results is clearly imaged anisotropy within the crust and uppermost mantle of Walker Lane, a region that accommodates roughly 25% of the relative plate boundary motion. It should also be made clear that the observed structure is not observed at all stations analyzed in Walker Lane. At stations FUR, GRA and SLA anisotropic structure is present and generally consistent between stations. At CWC and TIN anisotropic and/or dipping structure appears to be present but is significantly more complex and is not in agreement with FUR, GRA and SLA. Small scale regional complexities, including the presence of structural basins (Stevens et al., 2013) and melt in the mid-crust (Frasetto et al, 2011) may obscure similarities between the stations. Finally, MLAC showed highly complex structure, also likely the result of melt ponding in the crust.

5. Significance

The first goal of our proposed work was to characterize changes in the orientation of seismic anisotropy change from the lithosphere to the asthenosphere in southern California. While there is evidence at many stations to support the presence of anisotropy in the upper mantle at depths of ~ 70 km (8-12 seconds), it is rarely the first order feature observed in our work. Instead anisotropic structure appears most prominently at depths associated with the lower crust and uppermost mantle (4-8 seconds) (**Figure 2**) and because of significant complexity, we chose to focus our attention on shallower structure in this report. Future analysis on anisotropy at the plate-convecting mantle interface is critical for our understanding of the lithosphere-asthenosphere system more generally.

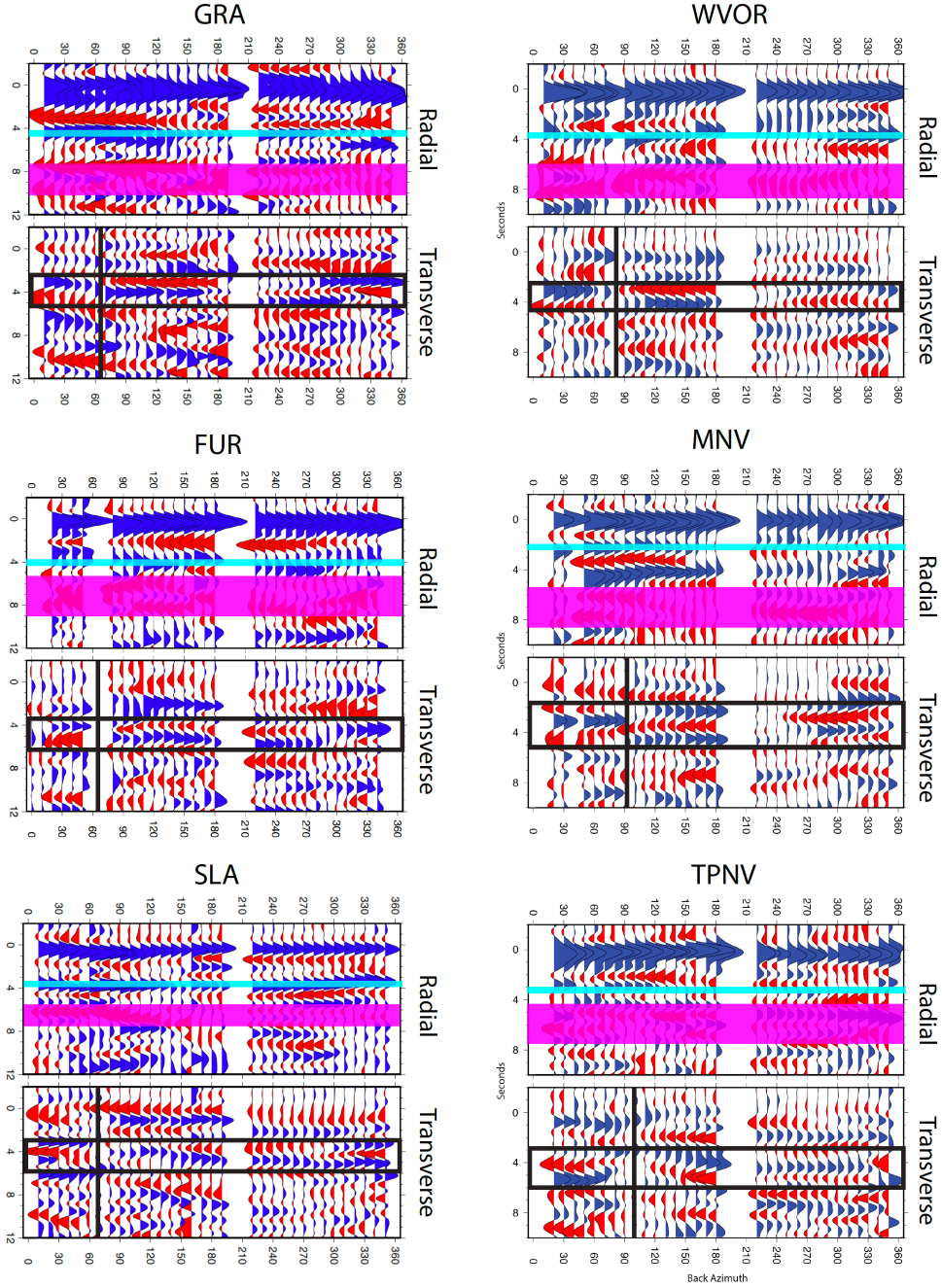


Figure 2. Radial (top panels) and Transverse (bottom panels) component P_s receiver functions calculated in this study (left column) and previously (right column). Receiver functions are binned as a function of back azimuth (shown on the x-axis) in 10degree increments and filtered to 1 Hz. Positive (blue) pulses correspond to a velocity increase with increasing depth and negative (red) pulses correspond to a velocity decrease with increasing depth. On the radial component RFs, the Moho arrival is highlighted with a semi-transparent blue line, and the LAB arrivals are highlighted with a semi-transparent magenta box. The transverse component receiver functions show significant complexity. A pair of phases with polarity reversals at ~4-6 seconds (highlighted with a black box) show similarities to receiver functions calculated during an earlier analysis of Basin and Range structure. Note that the back azimuth at which polarity reversals occur (vertical black line) is similar among all stations. A model of the anisotropic structure is shown in **Figure 3** and discussed in the text.

The second goal of our proposed work is to determine whether lateral variations in seismic anisotropy exist within the lithosphere across the plate boundary, and to see if we can make sense of them. Based on the work this study, and our previous work in central California and the Basin and Range, the answer is a definitive yes. Although not shown, Ps RF analysis shows pronounced variations in anisotropy on either side of the plate boundary and these observations are also supported by shear wave splitting analysis (Jiang et al., 2018). In this study, we observe the presence of a distinctive anisotropic signature beneath stations occupying the westernmost extent of the Basin and Range and/or Walker Lane. In Walker Lane, extension has lately evolved into a trans-tensional tectonic setting and may represent a nascent spreading center or plate boundary, similar to the proto-Gulf of California 12-6 Ma (Stevens et al., 2013). An important note is that not all stations in our earlier analysis of the Basin and Range showed such structure. Stations BMN and ELK, located in central Nevada, showed little to no evidence of anisotropy. The lack of observable anisotropy may be due to the presence of horizontally oriented mica, which would appear transversely isotropic (Erdman et al., 2013). Likewise, in our current analysis, stations CWC, TIN and MLAC were significantly more complex than the stations highlighted in Figure 2. While it is possible that the stations have similar structure located at depth, they are each located near a region which has experienced recent volcanism and have evidence for mid-crustal melt (Frassetto et al., 2011).

Previous modeling of data from station WVOR, demonstrated that dipping structure without anisotropy does not fit the data sufficiently well and one or more layers of anisotropy are required in the lower crust, and possibly an additional layer of anisotropy in the uppermost mantle, but it is not required. **Figure 3** demonstrates three possible models and includes the corresponding model RFs. More modeling work is required to understand the full range of deformation scenarios. If the dominant deformation is extension, phases such as mica should orient itself horizontally with the slow axis of symmetry being vertical, resulting in a transverse isotropy. Because we observe significant anisotropy in the lower crust either other mineral phase anisotropies must dominate, or mica is oriented in a direction other than vertical. While the two models shown in **Figure 3** fit the data well, they are not unique solutions and a more careful search of best fitting models is a future priority of this study.

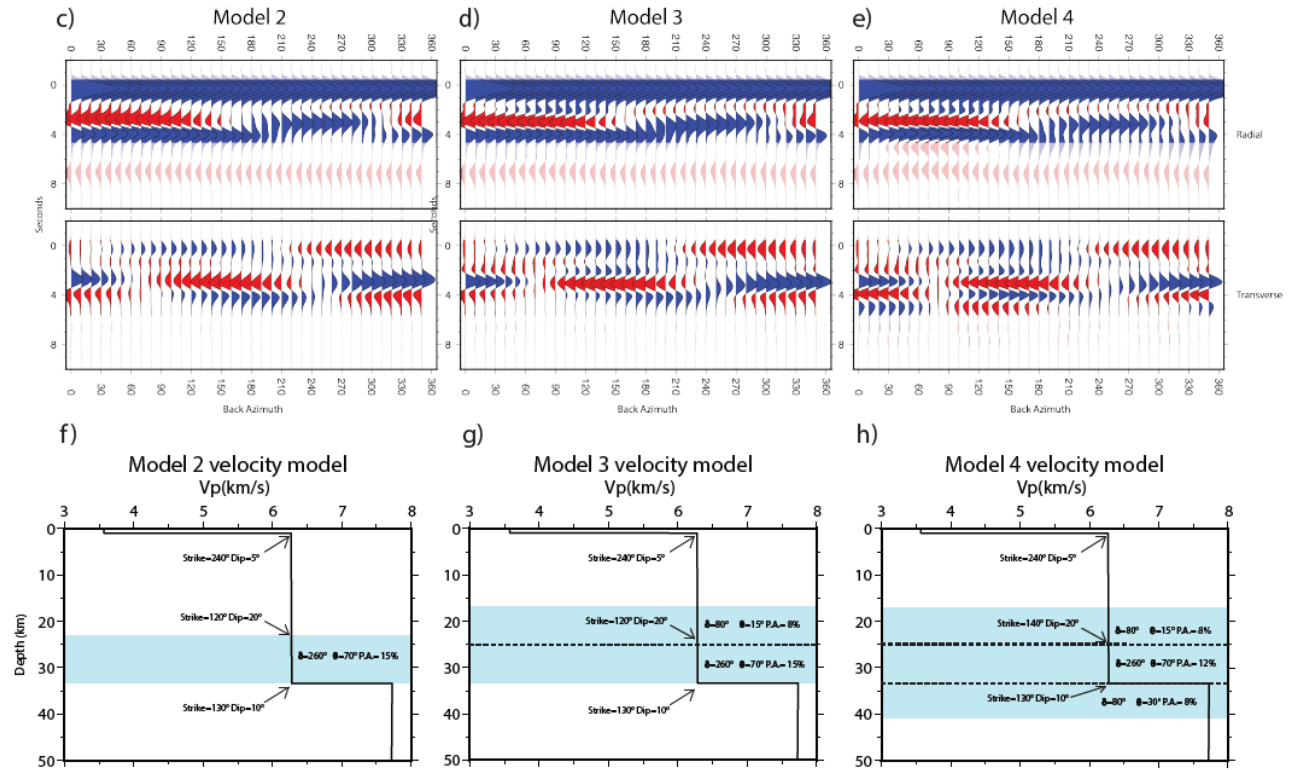


Figure 3. Model 2 contains one layer of anisotropy with dipping structure. Model 3 contains two layers of anisotropy in the lower crust with associated dipping structure. Model 4 contains dipping structure and three layers of anisotropy: two in the lower crust, and one in the mantle lithosphere.

References

- Abt, D. L., Fischer, K. M., French, S. W., Ford, H. A., Yuan, H. and Romanowicz, B. North American lithospheric discontinuity structure imaged by Ps and Sp receiver functions. *J. Geophys. Res.* **115**, B09301 (2010).
- Barak, S., & Klemperer, S. L. (2016). Rapid variation in upper-mantle rheology across the San Andreas fault system and Salton Trough, southernmost California, USA. *Geology*, *44*(7), 575-578.
- Bonnin, M., Barruol, G., and Bokelmann, G. H. R. Upper mantle deformation beneath the North American–Pacific plate boundary in California from SKS splitting. *J. Geophys. Res.* **115**, B04306 (2010).
- Bonnin, M., Tommasi, A., Hassani, R., Chevrot, S., Wookey, J., & Barruol, G. (2012). Numerical modelling of the upper-mantle anisotropy beneath a migrating strike-slip plate boundary: the San Andreas Fault system. *Geophysical Journal International*, *191*(2), 436-458.
- Bostock, M. G. Mantle stratigraphy and evolution of the Slave province. *J. Geophys. Res.* **103**, 21183-21, (1998).
- Eakin, C. M., Obrebski, M., Allen, R. M., Boyarko, D. C., Brudzinski, M. R., and Porritt, R. Seismic anisotropy beneath Cascadia and the Mendocino triple junction: Interaction of the subducting slab with mantle flow. *Earth Planet. Sci. Lett.* **297**, 627-632 (2010).
- Erdman, M. E., Hacker, B. R., Zandt, G., & Seward, G. Seismic anisotropy of the crust: electron-backscatter diffraction measurements from the Basin and Range. *Geophysical Journal International*, *195*(2), 1211-1229 (2013).
- Ford, H. A., Fischer, K. M., & Lekic, V. (2014). Localized shear in the deep lithosphere beneath the San Andreas fault system. *Geology*, *42*(4), 295-298.
- Ford, H. A., Long, M. D., & Wirth, E. A. (2016). Midlithospheric discontinuities and complex anisotropic layering in the mantle lithosphere beneath the Wyoming and Superior Provinces. *Journal of Geophysical Research: Solid Earth*, *121*(9), 6675-6697.
- Frassetto, A. M., Zandt, G., Gilbert, H., Owens, T. J., & Jones, C. H. Structure of the Sierra Nevada from receiver functions and implications for lithospheric foundering. *Geosphere*, *7*(4), 898-921 (2011).
- Frederiksen, A. W., and Bostock, M. G. Modelling teleseismic waves in dipping anisotropic structures. *Geophys. J. Int.* **141**, 401-412 (2002).
- Jiang, C., Schmandt, B., & Clayton, R. W. An anisotropic contrast in the lithosphere across the central San Andreas fault. *Geophysical Research Letters*, *45*, 3967–3975. <https://doi.org/10.1029/2018GL077476> (2018).
- Leahy, G. M., & Park, J. (2005). Hunting for oceanic island Moho. *Geophysical Journal International*, *160*(3), 1020-1026.
- Levin, V., and Park, J. P-SH conversions in layered media with hexagonally symmetric anisotropy: a cookbook. *Pure and applied geophysics* **151**, 669-697 (1998).
- Levin, V., and Park, J. P-SH conversions in a flat-layered medium with anisotropy of arbitrary orientation. *Geophys. J. Int.* **131**, 253-266 (1997).
- Lin, F., Ritzwoller, M. H., Yang, Y., Moschetti, M. P., and Fouch, M. J. Complex and variable crustal and uppermost mantle seismic anisotropy in the western United States. *Nature Geoscience* **4**, 55-61 (2010).

- Molnar, P. and Dayem, K. E. Major intracontinental strike-slip faults and contrasts in lithospheric strength. *Geosphere*, **6**, 444-467 (2010).
- Monteiller V. and Chevrot, S. High-resolution imaging of the deep anisotropic structure of the San Andreas Fault system beneath southern California. *Geophys. J. Int.* **186**, 418-446 (2011).
- Ozacar, A., and Zandt, G. Crustal structure and seismic anisotropy near the San Andreas Fault at Parkfield, California. *Geophys. J. Int.* **178**, 1098-1104 (2009).
- Porter, R., Zandt, G., & McQuarrie, N. (2011). Pervasive lower-crustal seismic anisotropy in Southern California: Evidence for underplated schists and active tectonics. *Lithosphere*, 3(3), 201-220.
- Plesch, A., Shaw, J. H., Benson, C., Bryant, W. A., Carena, S., Cooke, M., ... & Hauksson, E. (2007). Community fault model (CFM) for southern California. *Bulletin of the Seismological Society of America*, 97(6), 1793-1802.
- Rolandone, F., Bürgmann, Agnew, D. C., Johanson, I. A., d'Alessio, M. A., Titus, S. J., DeMets, C., and Tikoff, B. Aseismic slip and fault-normal strain along the central creeping section of the San Andreas fault. *Geophys. Res. Lett.* **35**, L14305 (2008).
- Savage, M. K. Lower crustal anisotropy or dipping boundaries? Effects on receiver functions and a case study in New Zealand. *J. Geophys. Res.* **103**, 15069-15 (1998).
- Schulte-Pelkum, V., Monsalve, G., Sheehan, A., Pandey, M. R., Sapkota, S., Bilham, R. and Wu, F. Imaging the Indian subcontinent beneath the Himalaya. *Nature* **435**, 1222-1225 (2005).
- Schulte-Pelkum, V., & Mahan, K. H. (2014). A method for mapping crustal deformation and anisotropy with receiver functions and first results from USArray. *Earth and Planetary Science Letters*, 402, 221-233.
- Schulte-Pelkum, V., & Mahan, K. H. (2014). Imaging faults and shear zones using receiver functions. *Pure and Applied Geophysics*, 171(11), 2967-2991.
- Stevens, C. H., Stone, P., & Blakely, R. J. Structural Evolution of the East Sierra Valley System (Owens Valley and Vicinity), California: A Geologic and Geophysical Synthesis. *Geosciences*, 3(2), 176-215 (2013).
- Wesnousky, S. G., Bormann, J. M., Kreemer, C., Hammond, W. C., & Brune, J. N. Neotectonics, geodesy, and seismic hazard in the Northern Walker Lane of Western North America: Thirty kilometers of crustal shear and no strike-slip?. *Earth Planet. Sci. Lett.* 329, 133-140 (2012).
- Yuan, H., & Levin, V. (2014). Stratified seismic anisotropy and the lithosphere-asthenosphere boundary beneath eastern North America. *Journal of Geophysical Research: Solid Earth*, 119(4), 3096-3114.